(5) CODATA Task Group on key values for thermodynamics, *J. Chem. Thermodyn.*, **3**, 1 (1971).
(6) Coops, J., van Nes, K., *Recl. Trav. Chim. Pays-Bas*, **66**, 131 (1947).
(7) Coops, J., van Nes, K., *Recl. Trav. Chim. Pays-Bas*, **66**, 161 (1947).
(8) Coops, J., van Nes, K., Kentie, A., Dienske, J. W., *Recl. Trav. Chim. Pays-Bas*, **66**, 113 (1947).
(9) Head, A. J., Good, W. D., Mosselman, C., in "Combustion Calorimetry", Vol. 1 in the series "Experimental Chemical Thermodynamics", S. Sunner and M. Månsson, Ed., Pergamon Press, London, Chapter 8, in press.
(10) Hubbard, W. N., Scott, D. W., Waddington, G., in "Experimental Thermochemistry," F. D. Rossini, Ed., Interscience, New York, N.Y., 1956, Chapter 5. Now out of print and superseded by the material of ref 11.
(11) Månsson, M., Chapter 5 in ref 9.
(12) Mosselman, C., Churney, K. L., Chapter 3 in ref 9.
(13) Mosselman, C., Dekker, H., *Recl. Trav. Chim. Pays-Bas*, **88**, 161 (1969).
(14) Mosselman, C., Dekker, H., *Recl. Trav. Chim. Pays-Bas*, **88**, 257 (1969).
(15) Rossini, F. D., Chapter 14 in ref 10.
(16) Svoboda, M., Yudin, A. T., Sicher, J., *Collect. Czech. Chem. Commun.*, **32**, 1625 (1967).

Received for review September 26, 1977. Accepted December 17, 1977.

Physical and Thermodynamic Properties of 1,1,2-Trifluorotrichloroethane (R-113)

Martin J. Mastroianni,* Richard F. Stahl, and Paul N. Sheldon

Specialty Chemicals Division, Allied Chemical Corporation, Buffalo, New York 14210

The critical temperature, vapor pressure, liquid densities, and *P–V–T* relations for R-113 were measured from 0.1 to 1.2 times the critical density. The physical properties were correlated to appropriate equations and consistent thermodynamic tables and graphs generated.

Introduction

The compound 1,1,2-trifluorotrichloroethane (R-113) is a well-known solvent and refrigerant. In recent years, there has been an increasing use of R-113 in high-temperature and high-pressure applications. A review of the thermodynamic properties shows that there is a lack of data in this region of interest. To assist designers in these applications, it was felt that improved and extended thermodynamic data should be developed. Thus, physical properties were measured, and a comprehensive thermodynamic table was generated.

The physical properties measured were the critical temperature, vapor pressure (from the freezing point to the critical temperature), liquid densities, and *P–V–T* relations from 0.1 to 1.2 times the critical density. The ideal heat capacities were obtained from the work of Higgens and Lielmezs (*7*). These values were corrected for the asymmetrical top contribution.

The thermodynamic properties were computed from the equations used to represent the physical properties of R-113 using thermodynamic relationships as described by Martin (*13*). The tables and graphs compiled are complete and thermodynamically consistent.

Experimental Work

(a) Sample Preparation. A sample of R-113 was distilled in a 5-ft vacuum-jacketed column with Podbielniak "Heli-Pak" packing. A heart cut, based on gas chromatography, was taken and a 1-kg sample obtained. The sample was dried, degassed (*15*) and vacuum transferred to an evacuated cylinder. A purity of 99.99+ (area %) was obtained as measured by gas chromatography and this sample was used for all the physical property measurements. All transfers were performed on a vacuum line to ensure a dry and air-free sample.

(b) Critical Temperature. The critical temperature was determined by observation of the meniscus in a sealed glass tube. The technique has been previously described (*15*). All temperatures were measured with a calibrated platinum resistance thermometer (U.S. National Bureau of Standards °C. Int., 1968) using a L&N "Speedomax" G resistance recorder to ±0.01 °C.

(c) Saturated Liquid Densities. The liquid densities were determined by a float technique which was found to be accurate to 0.1% over the range covered (*15*). The float density was corrected for the thermal expansion of glass from its calibration temperature at 23 °C.

(d) Vapor Pressure. The saturated vapor pressure was measured over the range from −22 °F to the critical temperature using three techniques. (1) At temperatures below room temperature and subatmospheric pressures, the vapor pressures were measured directly using a mercury manometer and a cathetometer. The accuracy of these measurements was better than 0.1%. (2) From temperatures just below room temperature to above room temperature and to about 25 psia, the vapor pressures were obtained by means of an isoteniscope and a mercury manometer. The accuracy of these measurements was better than 0.1%. (3) For high temperatures and pressures a calibrated null point pressure transmitter and balancing system was used (*15*, *17*). The balancing pressure was read on calibrated 16-in. Heise gauges (0–100, 0–300, and 0–1000 psi). Periodically pressures were checked with a Harwood controlled clearance pressure gauge. These gauges were accurate to 0.1% of the full scale reading. All samples were thermostated in liquid baths using various fluids at different temperatures or in an air oven which were controlled to ±0.02 and ±0.05 °F, respectively. The bath temperatures cycled over a time span

0021-9568/78/1723-0113$01.00/0

Table I. R-113 Vapor Pressure Equation Fit[a]

Temp, °R	Obsd pressure, psia	Calcd pressure, psia	% dev
428.670	0.3012	0.29913	0.687
437.526	0.4110	0.41246	−0.354
455.976	0.7623	0.76624	−0.520
473.598	1.3109	1.31454	−0.277
491.670	2.1782	2.1826	−0.202
509.688	3.4703	3.47123	−0.027
513.839	3.8581	3.84212	0.414
527.706	5.3358	5.32097	0.278
527.832	5.3388	5.33625	0.048
545.704	7.9086	7.88960	0.240
563.899	11.4097	11.40409	0.049
572.963	13.5616	13.56311	−0.011
582.523	16.172	16.1740	−0.012
596.781	20.765	20.7760	−0.053
601.31	22.40	22.431	−0.136
608.98	25.43	25.465	−0.137
617.92	29.35	29.387	−0.125
636.03	38.97	38.727	0.625
654.53	50.27	50.432	−0.323
672.10	63.69	63.832	−0.224
708.73	100.02	100.110	−0.090
741.04	142.99	143.144	−0.108
785.21	223.07	222.459	0.274
815.85	294.72	294.250	0.159
850.41	394.66	395.591	−0.236
837.86	479.65	479.914	−0.055

[a] Residual standard deviation ≈ 258 × 10^{-3}.

of from 20 to 30 min. The pressures and temperatures were read simultaneously, minimizing any effect of the bath control on the measurements.

(e) Pressure-Volume-Temperature Relationship. The $P-V-T$ properties of the superheated vapor were measured from saturation to 480 °F using a stainless steel constant volume apparatus (*15*).

To obtain the isochors, sample weights of from 20 to 250 g were transferred to the equipment from a tared cylinder. At the completion of the run, the charge was recovered in the tared cylinder. The initial and final weights agreed to 2 × 10^{-3} g. This gave a maximum uncertainty of 0.01%. Seven isochors (averaging six points each) were run from 0.1 to 1.2 times the critical density.

(f) Heat Capacity. The ideal heat capacity of R-113, $C_p°$, was taken from the values given by Higgens and Lielmezs (*7*). These values were corrected for the asymmetrical top contribution and showed good agreement with the recent data of Ernst and Busser (*6*).

Experimental Results

(a) Critical Properties. The critical temperature, obtained from the average temperature at which the meniscus disappeared and reappeared, was T_c = 417.8 °F. Benning and McHarness (*2*) obtained a temperature of 417.4 °F. When our temperature was used in the vapor pressure equation, a critical pressure P_c = 494.7 psia was obtained. Benning and McHarness (*2*) obtained a pressure (P_c) of 495.4 psia. The critical density was determined from a rectilinear plot as D_c = 35.58 lb/ft^3. A critical density of 35.96 lb/ft^3 was obtained by Benning McHarness (*2*).

(b) Vapor Pressure. The laboratory data were fitted with the equation

$$\ln P = A + B/T + CT + DT^2 + (E)\,[(F-T)/T]\ln(F-T) \quad (1)$$

Table II. R-113 Vapor Pressure Comparisons

Temp, °R	P-allied eq, psia	P(exptl), psia	% dev	Ref source
455.81	0.5511	0.5452	−1.07	9
476.55	1.4623	1.4623	+1.77	7
491.67	2.1880	2.1133	−3.41	14
527.22	5.2678	5.2538	−0.27	9
527.67	5.3220	5.7972	+8.93	10
527.67	5.3220	5.2700	−0.98	14
572.58	13.459	14.054	+4.42	10
577.30	14.692	14.696	+0.02	7
601.76	22.572	22.528	−0.19	9
634.32	37.69	37.67	−0.05	9
641.61	41.94	42.49	+1.31	7
723.33	117.86	118.86	−0.85	7
870.79	467.64	473.80	+1.32	7

Table III. R-113 Liquid Density Equation Fit[a]

Temp, °R	Obsd density, lb/ft^3	Calcd density, lb/ft^3	% dev
506.62	99.900	99.8924	0.0081
582.89	93.620	93.6231	−0.0033
652.26	87.346	87.3758	−0.0343
713.78	81.078	81.0772	0.0008
765.58	74.822	74.7599	0.0836
806.07	68.573	68.5538	0.0282
835.79	62.330	62.4768	−0.2353
857.57	56.087	55.9622	0.2226
869.78	49.857	49.8934	−0.0739

[a] Standard deviation ≈ 73.9 × 10^{-3}.

Table IV. R-113 Liquid Density Comparison with Literature Values

Temp, °R	Density allied eq, lb/ft^3	Density exptl, lb/ft^3	% dev	Source
437.67	105.25	105.37	0.08	9
491.67	101.08	101.11	0.03	14
491.67	101.08	101.20	0.12	9
635.67	88.925	89.163	0.27	9
715.23	80.926	81.065	0.17	6
810.63	67.898	67.649	−0.37	6
851.43	56.667	55.962	−1.23	6

where P = psia, T = °R, A = 23.428 348 (more than the logical number of significant figures are given to permit exact checking of computer programs), B = 9059.6033, C = −0.0125 548 570, D = 5.339 122 7 × 10^{-6}, E = 0.140 257 95, and F = 878.484 16. The predicted pressures for this equation and the experimental data are given in Table I. The literature contains several sets of experimental data on the vapor pressure of R-113 (*3*, *8*, *14*). However, the agreement is not good. The best data appeared to be that of Ridel (*14*) and Benning and McHarness (*2*). The data of Hiraoka and Hildebrand (*8*) seem to be in serious error. The predictions of this equation are compared with data from the literature in Table II.

(c) Saturated Liquid Density. The liquid density data were fitted to the following equation:

$$\text{density} = D_{cr} + (A_d)(X) + (B_d)(X^2) + C_d(X^3) + (D_d)(X^4) \quad (2)$$

Table V. Correlation of P-V-T Data Using Martin-Hou Equation of State

Volume, ft³/lb	Temp, °R	Obsd pressure, psia	Calcd pressure, psia	% dev
0.286 587	728.37	119.36	119.14	0.183
0.286 667	754.58	126.24	125.74	0.394
0.286 731	779.96	132.55	132.00	0.413
0.286 803	804.11	137.72	137.85	−0.092
0.286 883	834.98	145.22	145.19	0.021
0.286 955	860.22	151.01	151.10	−0.057
0.287 187	944.71	170.37	170.42	−0.027
0.092 277	830.11	320.36	322.33	−0.614
0.092 295	851.72	342.00	342.93	−0.273
0.092 318	878.27	366.56	367.62	−0.289
0.092 347	907.58	392.96	394.18	−0.311
0.092 367	930.78	413.96	414.79	−0.201
0.092 385	952.94	433.08	434.18	−0.254
0.055 547	869.31	446.15	446.06	0.020
0.055 557	888.10	480.55	479.81	0.154
0.055 567	905.72	511.04	510.91	0.026
0.055 578	925.76	546.28	545.67	0.111
0.055 588	945.00	578.78	578.54	0.041
0.055 595	957.78	600.98	600.12	0.143
0.039 712	873.86	479.65	480.23	−0.122
0.039 714	881.10	501.76	500.36	0.279
0.039 721	896.60	544.21	543.05	0.214
0.039 727	914.63	592.80	592.08	0.122
0.039 734	932.49	640.17	640.01	0.026
0.039 742	881.91	512.30	511.07	0.241
0.030 913	952.58	692.82	693.26	−0.050
0.030 918	899.48	577.76	576.54	0.211
0.030 923	914.26	631.52	631.31	−0.033
0.030 927	931.19	692.59	693.78	−0.172
0.030 931	943.74	740.16	739.86	0.041
0.030 931	958.32	792.38	793.25	−0.110
0.027 694	895.82	570.71	572.11	−0.245
0.027 699	913.09	643.90	645.14	−0.193
0.027 703	927.68	706.47	706.93	−0.065
0.027 709	951.84	809.48	809.20	0.036
0.027 714	968.74	881.90	880.77	0.129
0.023 316	878.90	503.33	502.74	0.117
0.023 320	897.41	598.50	599.99	−0.249
0.023 323	915.08	693.38	694.45	−0.154
0.023 326	927.40	760.42	761.05	−0.082
0.023 330	943.94	851.72	851.45	0.031
0.023 332	952.58	900.28	899.07	0.135

where density = lb/ft³, $X = (1 - T/Tc)^{1/3}$, T = °R, T_c = 877.52 °R, D_α = 35.5850 lb/ft³, A_d = 58.448 694, B_d = 69.272 809, C_d = −96.262 521, D_d = 69.721 905.

The measured and calculated values are given in Table III ($APD = 0.767 \times 10^{-1}$). The predictions of the above equation are compared with data from the literature in Table IV.

(d) P-V-T Relationship. The P-V-T properties of the superheated vapor were measured from saturation to 480 °F and up to pressures of 1000 psia. The isochors were run at 0.1, 0.3, 0.5, 0.7, 0.9, 1.0, and 1.2 times the critical density. The data were correlated with the Martin–Hou equation of state (*11*, *12*).

$$P = \sum_{i=1}^{5} f_i(V-b)^{-i} \qquad (3)$$

where $f_i = A_i + B_i \times T + C_i e^{-KT/T_c}$, P = psia, V = ft³/lb, T = °R, $A_1 = C_1 = B_4 = C_4 = 0$, B_1 = R, $b = 0.679\,030 \times 10^{-2}$, $B_1 = 0.572\,727\,7 \times 10^{-1}$, $K = 5.475\,000$, $T_c = 877.52$, $A_2 = -2.736\,234$, $B_2 = 0.102\,313\,6 \times 10^{-2}$, $C_2 = -49.978\,04$, $A_3 = 0.047\,067\,47$, $B_3 = -0.115\,918\,0 \times 10^{-4}$, $C_3 = 1.182\,675$, $A_4 = -4.291\,722 \times 10^{-4}$, $A_5 = 0.412\,583\,3 \times 10^{-8}$, $B_5 = 0.180\,485\,1 \times 10^{-8}$, and $C_5 = -0.546\,164\,4 \times 10^{-4}$. Table V gives the predicted and experimental values with a residual standard deviation of 881.0×10^{-3}.

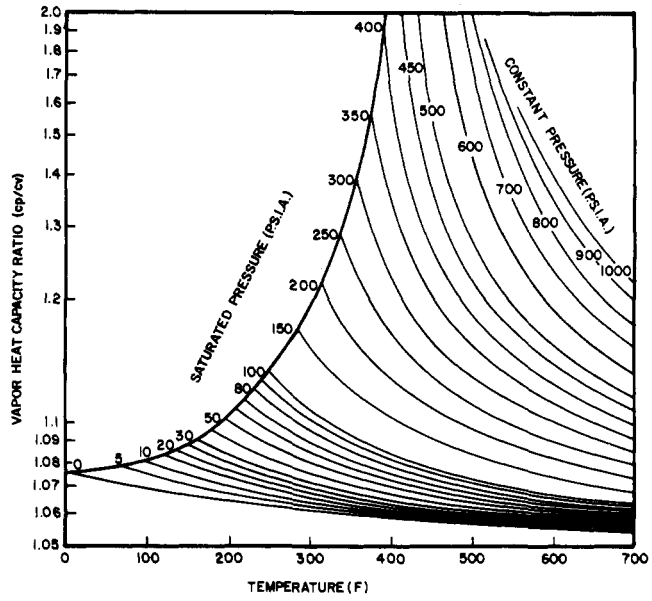

Figure 1. R-113 vapor heat capacity ratio (C_p/C_v).

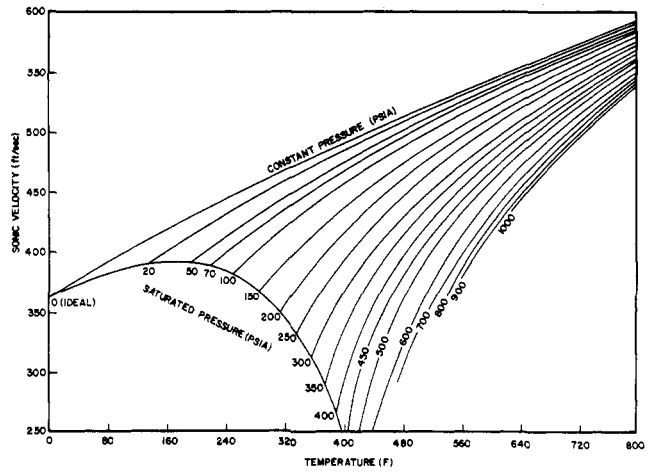

Figure 2. R-113 sonic velocity.

(e) Heat Capacity. The ideal heat capacity equation obtained from the above data of Higgens and Lielmezs (*7*) corrected for asymmetrical top contribution is as follows:

$$C_p^\circ = A_c + B_cT + C_cT^2 + D_cT^3 + E_cT^4 \qquad (4)$$

T = °R, C_p = btu/(lb-mol °R), A_c = 6.587 111, B_c = 0.068 373 91, $C_c = -5.624\,147 \times 10^{-5}$, $D_c = 2.251\,297 \times 10^{-8}$, and $E_c = -3.549\,403 \times 10^{-12}$.

(f) Thermodynamic Tables. The equations (1–4) representing the physical properties of R-113 were used to define a complete thermodynamic network. These empirical equations were put into the thermodynamic relations and the thermodynamic properties computed (*13*).

The computations resulted in tables and graphs over a temperature range of −35 to +800 °F and a pressure range of 0.1–1000 psia. Abbreviated forms of the saturated and superheat tables are presented here in Tables VI and VII to indicate the nature of the final results. The ratio of C_p/C_v as a function of P and T is shown in Figure 1 and the velocity of sound as a function of P and T is given in Figure 2. A large scale (11 × 17 in.) pressure–enthalpy chart has been constructed presenting the data covered by the tables. This chart is shown in reduced form in Figure 3.

Thermodynamic properties of great reliability can be calculated with three groups of computer programs, when complete

Table VI. Thermodynamic Properties of Saturated R-113

Temp, °F	Pressure, psia	Volume, ft³/lb		Enthalpy, btu/lb			Entropy, btu/(lb °F)	
		Liquid	Vapor	Liquid	Latent	Vapor	Liquid	Vapor
−35.00	0.2599	0.009 413	93.380 39	0.993	71.842	72.835	0.002 35	0.171 51
−20.00	0.4473	0.009 515	56.118 36	4.002	71.001	75.003	0.009 31	0.170 79
0.00	0.8657	0.009 565	30.244 49	8.090	69.848	77.937	0.018 40	0.170 35
20.00	1.5727	0.009 803	17.319 90	12.263	68.652	80.915	0.027 29	0.170 41
40.00	2.7032	0.009 956	10.451 00	16.530	67.397	83.928	0.036 00	0.170 88
60.00	4.4268	0.010 117	6.599 86	20.878	66.090	86.968	0.044 52	0.171 69
80.00	6.9474	0.010 285	4.335 76	25.308	64.718	90.026	0.052 88	0.172 79
100.00	10.502	0.010 463	2.947 96	29.817	63.278	93.094	0.061 07	0.174 13
120.00	15.359	0.010 651	2.065 09	34.406	61.760	96.166	0.069 11	0.175 65
140.00	21.812	0.010 851	1.484 85	39.063	60.168	99.231	0.076 99	0.177 32
160.00	30.179	0.011 064	1.092 10	43.787	58.496	102.283	0.084 71	0.179 10
180.00	40.799	0.011 293	0.819 16	48.573	56.740	105.313	0.092 273	0.180 97
200.00	54.028	0.011 540	0.624 82	53.428	54.884	108.312	0.099 70	0.182 90
220.00	70.244	0.011 809	0.483 54	58.339	52.930	111.269	0.106 99	0.184 86
240.00	89.839	0.012 105	0.378 69	63.319	50.851	114.171	0.114 14	0.186 82
260.00	113.23	0.012 434	0.299 52	68.367	48.636	117.003	0.121 18	0.188 76
280.00	140.86	0.012 804	0.238 64	73.503	46.240	119.743	0.128 13	0.190 64
300.00	173.22	0.013 229	0.191 08	78.742	43.621	122.363	0.135 02	0.192 44
320.00	210.82	0.013 728	0.153 31	84.117	40.707	124.824	0.141 88	0.194 09
340.00	254.26	0.014 333	0.122 77	89.681	37.381	127.062	0.148 78	0.195 53
360.00	304.23	0.015 104	0.097 57	95.516	33.460	128.976	0.155 82	0.196 64
380.00	361.53	0.016 170	0.076 15	101.786	28.573	130.360	0.163 18	0.197 20
400.00	427.26	0.017 909	0.056 78	108.902	21.779	130.681	0.171 31	0.196 64
420.00	503.46	0.025 202	0.031 01	120.875	3.977	124.852	0.184 72	0.189 24

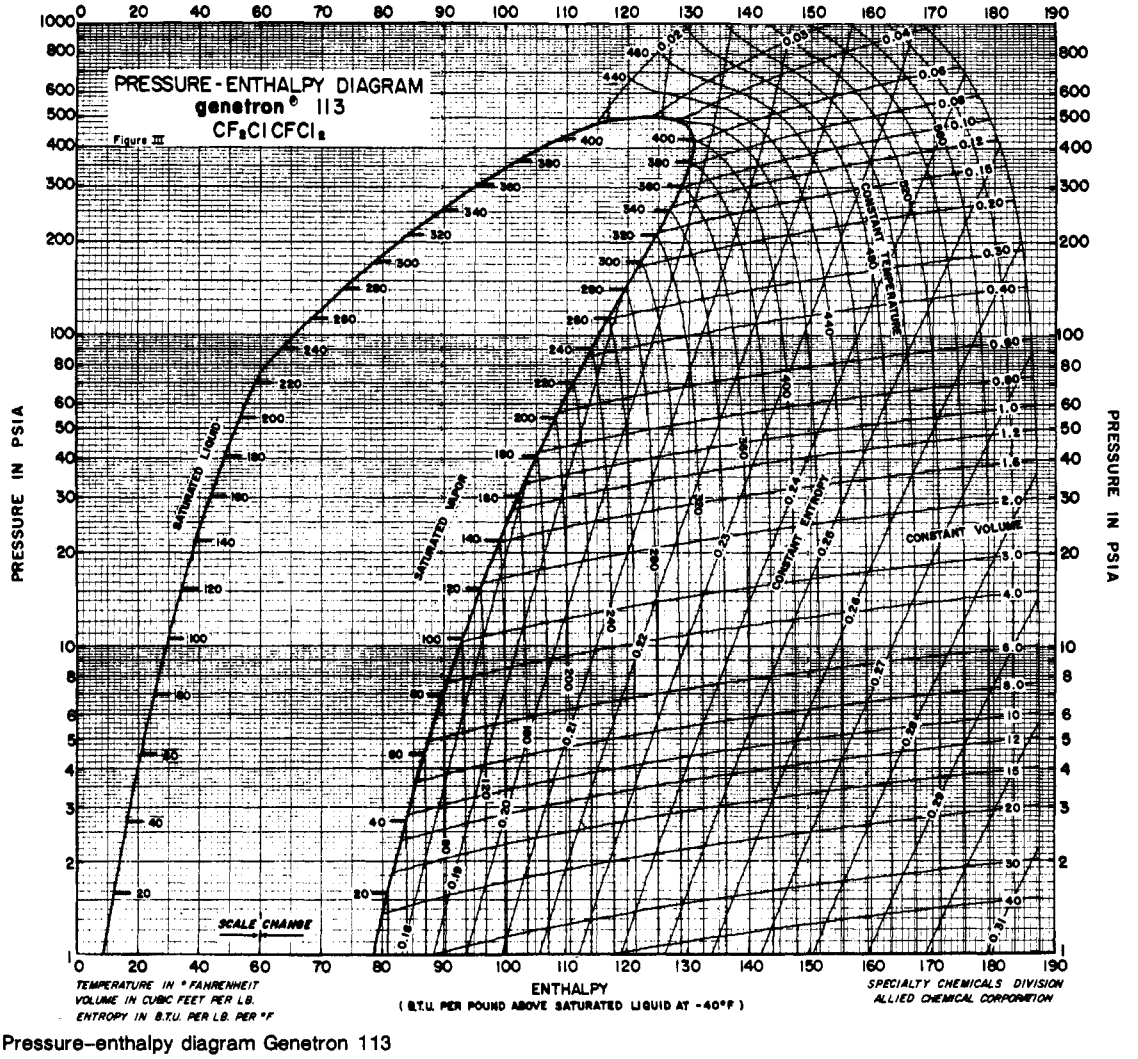

Figure 3. Pressure–enthalpy diagram Genetron 113

physical property measurements are made. The data required are (a) molecular weight, (b) critical point data (T_c, P_c, V_c), (c) vapor pressure, (d) ideal gas heat capacities, (e) liquid densities, and (f) $P-V-T$ measurements.

The critical temperature was measured, the critical volume estimated from a rectilinear diameter plot, and the critical pressure was computed from the vapor pressure correlation. The other physical properties were measured and correlated

Table VII. Thermodynamic Properties of Superheated R-113

P, psia	Units[a]	20 °F	60 °F	100 °F	140 °F	180 °F	220 °F	260 °F	300 °F	340 °F	380 °F
0.6	V	45.639	49.485	53.323	57.158	60.988	64.816	68.642	72.467	76.291	80.107
	H	81.011	87.276	93.763	100.453	107.332	114.383	121.593	128.948	136.437	144.048
	S	0.18076	0.19330	0.20533	0.21687	0.22797	0.23866	0.24897	0.25892	0.26852	0.27781
1.0	V	27.324	29.642	31.953	34.260	36.564	38.864	41.163	43.461	45.747	48.053
	H	80.972	87.244	93.737	100.432	107.313	114.367	121.579	128.936	136.426	144.038
	S	0.17529	0.18785	0.19988	0.21143	0.22254	0.23323	0.24354	0.25349	0.26310	0.27239
4.0	V		7.3174	7.9112	8.5003	9.0857	9.6685	10.249	10.829	11.407	11.984
	H		87.002	93.538	100.266	107.174	114.248	121.476	128.846	136.346	143.967
	S		0.17282	0.18493	0.19654	0.20769	0.21841	0.22875	0.23871	0.24833	0.25763
10.0	V			3.1014	3.3470	3.5893	3.829	4.0662	4.3020	4.5368	4.7706
	H			93.129	99.928	106.890	114.006	121.267	128.663	136.185	143.823
	S			0.17469	0.18642	0.19766	0.20845	0.21883	0.22883	0.23848	0.24780

P, psia	Units[a]	260 °F	300 °F	340 °F	380 °F	420 °F	460 °F	500 °F	540 °F	580 °F	620 °F
100	V	0.34920	0.38135	0.41145	0.44008	0.46775	0.49466	0.52099	0.54687	0.57240	0.59765
	H	117.646	125.600	133.540	141.503	149.507	157.560	165.668	173.831	182.049	190.321
	S	0.19075	0.20151	0.21170	0.22141	0.23072	0.23968	0.24830	0.25664	0.26470	0.27251
200	V			0.16597	0.19615	0.21360	0.22981	0.24520	0.25997	0.27427	0.28823
	H			125.399	138.424	146.877	155.264	163.630	171.999	180.385	188.797
	S			0.19524	0.21133	0.22117	0.23049	0.23940	0.24794	0.25616	0.26410
800	V						0.02028	0.03077	0.04124	0.04921	0.05584
	H						125.457	142.603	156.347	167.618	177.885
	S						0.18846	0.20670	0.22075	0.23181	0.24150

[a] Thermodynamic units: V, volume, ft³/lb; H, enthalpy, btu/lb; S, entropy, eu.

Table VIII. R-113 Critical Properties

	Allied	Benning and McHarness (2)	Hovorka (9)
P_c, psia	494.7	495.4	
d_c, lb/ft³	35.58	35.96	
T_c, °R	877.5	877.1	829.4

with various equations (using a Xerox Sigma 7 computer) described below.

$P-V-T$ data were correlated with the Martin–Hou equation of state (*13*), eq 3. The six-constant vapor pressure equation was used to correlate the saturated vapor pressure rather than a four-constant equation because of its ability to represent the data better in the vicinity of the critical region.

The first set of programs was used to correlate physical property data. Once the $P-V-T$, vapor pressure, and liquid density were correlated, the estimate of V_c was improved by plotting the average of the liquid and vapor densities as a function of temperature (rectilinear diameter plot) (*4*). A straight line is fitted and extrapolated to T_c for a new estimate of the critical density, D_{cr}. The liquid densities are refit and the entire procedure is repeated until no change in D_{cr} results, usually one cycle. Then the $P-V-T$ data are refit to the equation of state.

A second group of computer programs was utilized for calculating and printing (and microfiche) the thermodynamic tables. In addition to control cards, the table generating computer programs required property cards and pressure–temperature cards as input. The property cards contain (a) vapor pressure, (b) slope of the vapor pressure line, (c) liquid density (for saturated-state calculations), (d) ideal enthalpy, and (e) the ideal entropy at each temperature for which results are desired.

The pressure–temperature cards contain a pressure and a temperature range (initial, final, and increment) for results in the superheated region. Computer programs that accept pressure or temperature ranges and coefficients for the physical property correlations were used to punch the required property and pressure–temperature cards. After the thermodynamic table generating programs were run, the results were stored on two magnetic tapes until they were checked for accuracy. One tape had special format controls so that it was compatible for microfiche copy.

The last group of computer programs was used to produce a pressure–enthalpy diagram and tables of ideal gas heat capacities and sonic velocities. The inputs required are the coefficients for the various physical property correlation equations and some control information. The pressure–enthalpy diagram was plotted on a Calcomp 30″ plotter.

Discussion and Conclusions

There are four other sources of physical properties for R-113: Benning and McHarness (*2*, *3*), Riedel (*14*), Hiraoka and Hildebrand (*8*), and Hovorka and Geiger (*9*). A comparison of vapor pressures is given in Table V and it can be seen that the present work agrees well with that of Riedel and within about 1% to Benning and McHarness. Hiraoka and Hildebrand (*8*) differ greatly from the present work and the other published data.

Liquid densities are compared with other sources (*2*, *9*, *14*) in Table III and agree closely with the published data except at the low density end.

A comparison of critical properties is given in Table VIII where the present data compare quite well with those of Benning and McHarness (*2*). The critical temperature obtained by Hovorka and Geiger (*9*) is much lower.

A comparison of $P-V-T$ data is difficult as there is very little overlap. A data point that lies within the work done by Benning and McHarness (*1*) agrees to within 0.7% of their equation. The major portion of this work extends the range into higher densities, pressures, and temperatures.

This work has resulted in new thermodynamic tables that have an expanded range based on sound experimental data.

Acknowledgment

The authors wish to thank Mr. E. A. E. Lund and Mr. J. B. Moore for their assistance in collecting the physical properties. Thanks are also due to Dr. E. Rosenthal for applying computer programs, developed for earlier work, in computation of constants for the various equations, correlating the data, and producing the thermodynamic tables.

Glossary

A-F	constants in vapor pressure equation
A_d, B_d, C_a, D_d	constants in liquid density equation
A_i, B_i, C_i, b	constants in $P-V-T$ equation
A_c-E_c	constants in heat capacity equation
C_P	ideal heat capacity of gas btu/(lb/mol °R)
D_{cr}	critical density lb/ft^3
H	enthalpy, btu/lb
K	constant in $P-V-T$ equation
P	absolute pressure lb/in.^{2}
R	gas constant
S	entropy
T	absolute temperature, °R
T_c	critical temperature, °R
V	volume, ft^3/lb

Literature Cited

(1) Benning, A. F., McHarness, R. C., *Ind. Eng. Chem.*, **32**, 497–499 (1940).
(2) Benning, A. F., McHarness, R. C., *Ind. Eng. Chem.*, **32**, 698 (1940).
(3) Benning, A. F., McHarness, R. C., *Ind. Eng. Chem.*, **32**, 814 (1940).
(4) Cailletet, Mathias, *J. Phys.*, **5**, 549 (1886).
(5) Douslin, D. R., Morre, R. T., Dawson, J. P., Waddington, G., *J. Am. Chem. Soc.*, **80**, 2031 (1958).
(6) Ernst, G., Busser, J., *J. Chem. Thermodyn.*, **2**, 787–791 (1970).
(7) Higgins, E. R., Lielmezs, J., *J. Chem. Eng. Data*, **10**, 178–179 (1965).
(8) Hiraoka, H., Hildebrand, J. M., *J. Phys. Chem.*, **67**, 916 (1963).
(9) Hovorka, F., Geiger, F., *J. Am. Chem. Soc.*, **55**, 4759–4761 (1933).
(10) Martin, J. J., Hou, Y. C., *AIChE J.*, **5**, 125–129 (1959).
(11) Martin, J. J., Hou, Y. C., *AIChE J.*, **1**, 142 (1959).
(12) Martin, J. J., Kapoor, R. M., DeNevers, N., *AIChE J.*, **5**, 1959 (1959).
(13) Martin, J. J., *Am. Soc. Mech. Eng.* [*Pap.*], 110 (1959).
(14) Ridel, L., *Z. Gesamte Kaelte-Ind.*, **45**, 221–225 (1938).
(15) Sinka, J. V., Murphy, K. P., *J. Chem. Eng. Data*, **12**, 315 (1967).
(16) Speciality Chemicals Division, Allied Chemical Corp.
(17) White, D., Hilsenrath, J., *Rev. Sci. Instrum.*, **29**, 648 (1958).

Received for review November 23, 1976. Accepted January 30, 1978.

Vapor Pressure of Aluminum Chloride Systems. 2. Pressure of Unsaturated Aluminum Chloride Gas

John T. Viola, Armand A. Fannin, Jr., Lowell A. King,* and David W. Seegmiller

Frank J. Seiler Research Laboratory (Air Force Systems Command) and Department of Chemistry and Biological Sciences, United States Air Force Academy, Colorado 80840

The pressures and volumes of unsaturated, gaseous samples of aluminum chloride were measured from 167 to 277 °C. The samples were contained in a variable-volume Pyrex isoteniscope which utilized mercury as the manometric fluid. The mercury columns were brought to null by an external pressure which was in turn measured at each experimental point. The experimental values of temperature, pressure, and volume were fit to a van der Waals equation of state, giving $a = 4.285 \times 10^{10}$ cm^6 Torr mol^{-2} and $b = 178.9$ cm^3 mol^{-1}.

As part of an investigation of certain low-melting, molten salt electrolytes for high-energy density batteries, we needed to know the vapor density and vapor pressure of aluminum chloride. We have made these measurements for aluminum chloride vapor in equilibrium with the liquid or solid (*4*, *6*, *8*). Only a few measurements have been made on unsaturated gaseous aluminum chloride (*2*, *7*, *9*); these were concerned with determining the dissociation constant for the reaction $Al_2Cl_6(g) \rightleftarrows 2AlCl_3(g)$ and were made at higher temperatures than were of interest in the present work.

Experimental Section

Crystals of aluminum chloride were loaded into the Pyrex isoteniscope shown in Figure 1. Preparation of the aluminum chloride, loading of the isoteniscope, and the constant temperature bath and its temperature regulation and measurement were all as described previously (*8*). Sample pressures were also determined as before (*8*), but the external pressures were read by the capacitance manometer only in the present work.

Five samples of Al_2Cl_6 were used. The masses of samples I through V were 0.2512, 0.5790, 0.5978, 0.7499, and 1.0430 g, respectively. Estimated uncertainty in mass was ±0.0002 g. It was necessary to know not only the gas volume above each index mark on the bulb but also the total amount of mercury below each index mark, including the mercury in the two side arms. Additionally, the volume changes per unit length for the center compartment in the vicinity of each index mark and for the left-hand side arm were required. These volume calibrations were made by recording heights and weighing the apparatus when it contained varying amounts of water or mercury. These calibration data are given in Table I.

Measurements were made according to the following procedure. The evacuated isoteniscope (without mercury) and sample crystal were manipulated so that the crystal rested on the sample shelf. The isoteniscope was then immersed in a room temperature bath and connected to the pressure measurement device. Enough mercury was introduced to block the entrance to the middle compartment, and the bath was warmed to the desired beginning temperature. It was necessary to add mercury from time to time as the Al_2Cl_6 pressure increased. At the measurement temperature, internal pressure was sufficient to maintain a continuous column of mercury from the inner bulb to the stopcock at the mercury reservoir. The initial measurement was made on each sample by carefully admitting just enough mercury to cause the mercury columns to be at the